Influence of heteroepitaxy on the width and frequency of the E_2 (high)-phonon line in GaN studied by Raman spectroscopy

M. Giehler,[a] M. Ramsteiner, P. Waltereit, O. Brandt, and K. H. Ploog
Paul-Drude-Institut für Festkörperelektronik, Hausvogteiplatz 5-7, 10117 Berlin, Germany

H. Obloh
Fraunhofer-Institut für Angewandte Festkörperphysik, Tullastr. 72, 79108 Freiburg, Germany

(Received 28 August 2000; accepted for publication 13 December 2000)

Wurtzite GaN layers are commonly grown heteroepitaxially on 6H–SiC or Al_2O_3 substrates, because of the lack of lattice-matched substrates. We study the influence of these substrates mainly on the E_2(high)-phonon Raman line by temperature dependent Raman spectroscopy. We find that the line broadening with sample heating is predominantly caused by intrinsic phonon–phonon scattering in GaN. The small three-phonon contribution as well as the small intrinsic linewidth at low temperature are due to the rather low two-phonon density of states at the E_2(high)-phonon energy. Substrates with large lattice mismatch cause inhomogeneous strain and defects in the layers, which lead to a large, temperature independent, line broadening. We show that the temperature shift of the E_2(high)-phonon frequency is dominated by the GaN lattice expansion. The lattice of epilayers is strongly modified by the thermal in-plane expansion of the substrate. The degree of relaxation at the growth temperature is reflected by deviation of the E_2(high)-line from the intrinsic phonon frequency. © *2001 American Institute of Physics.* [DOI: 10.1063/1.1347406]

I. INTRODUCTION

Commonly, wurtzite GaN layers are grown heteroepitaxially on Al_2O_3 and 6H–SiC substrates, because of the lack of lattice-matched materials. The large lattice mismatch between these substrates and GaN as well as different thermal expansion coefficients lead to numerous defects and strain in the epitaxial layers. Strain influences mainly the frequency, whereas lattice defects reduce the phonon lifetime, which increases the width of the Raman lines. Therefore, the Raman spectroscopy of phonons is a powerful method for the characterization of heteroepitaxially grown layers.

From the Raman-active A_1(TO), A_1(LO), E_1(TO), E_1(LO), and E_2 phonons, the E_2(high)-line is the strongest one. It is observable in different scattering configurations. Therefore, in many publications,[1–5] this line is used to characterize heteroepitaxially grown wurtzite GaN layers. In order to compare different GaN layers, the width and position of the E_2(high)-line are commonly measured only at room temperature.[1–3] In this case temperature dependent and independent contributions to the linewidth or frequency cannot be separated. Kozawa *et al.*,[1] e.g., investigated the influence of the layer thickness of the position and width of the E_2(high)-line at 300 K. They observed a broadening and blueshift with decreasing layer thickness and interpret this as being due to inhomogeneously strained layers. However, the intrinsic linewidth of *ideal* GaN (and therewith an absolute value of the layer quality) have not yet been determined. Kisielowski *et al.*[2] and Klose *et al.*[3] carried out strain-related studies of films grown on SiC as well as Al_2O_3 substrates at room temperature. From these measurements the relaxation state of the layer at the growth temperature can only be roughly estimated, but such information is important, e.g., for the study of particular growth modes of GaN layers.[4] Furthermore, from room temperature measurements the bare phonon frequencies cannot be determined.

Detailed studies of the variation of internal strain in GaN epilayers as a function of temperature and of the phonon anharmonicity in GaN have not been published. In this article, we study the temperature dependence of the width and shift of the E_2(high)-Raman line of hexagonal GaN layers grown on Al_2O_3 and 6H–SiC substrates. In our analysis of the experimental data, we take into account anharmonic phonon–phonon interactions as well as the volume change of the GaN lattice due to the thermal expansion of GaN itself, the thermal properties of the substrates, and the relaxation of the layers. We consider two aspects. First, we determine the intrinsic anharmonicity parameters of the E_2(high) and A_1(LO) phonons including the bare phonon frequencies from heteroepitaxially grown layers. Second, for the characterization of epilayers, we derive simple equations describing the temperature dependent broadening and shift of the E_2(high)-Raman line for both considered substrates. These equations also contain phenomenological parameters in order to take into account, e.g., line broadening due to inhomogeneous strain and crystalline defects in the layers or the influence of an incomplete layer relaxation on the phonon frequencies.

In Sec. II, the basic equations are given, which describe the anharmonic phonon–phonon interactions. In particular, we use a slightly modified Grüneisen equation which describes well the temperature shift of heteroepitaxially grown layers. In Sec. III the samples as well as the experiments are

[a]Author to whom correspondence should be addressed; electronic mail: giehler@pdi-berlin.de

described. The experimental results are shown in Sec. IV and analyzed in Sec. V regarding phonon–phonon scattering, temperature independent phonon line broadening contributions, and the effect of lattice expansion and relaxation on the phonon frequency. Finally, Sec. VI summarizes the results and gives some conclusions.

II. PHONON ANHARMONICITY

A. Raman scattering

The line shape of the first-order Stokes Raman peak at low temperature ($kT \ll \hbar\omega$) is given by[6,7]

$$I(\mathbf{0}j,\omega) \propto \frac{\Gamma^2(\mathbf{0}j,\omega)}{[\omega-\omega_0(\mathbf{0}j)-\Delta(\mathbf{0}j,\omega)]^2+\Gamma^2(\mathbf{0}j,\omega)}, \quad (2.1)$$

where ω denotes the frequency, $\mathbf{q}\approx\mathbf{0}$ the zone-center wave vector, j the phonon branch [E_2(high) and A_1(LO) in our case], and $\omega_0(\mathbf{0}j)$ is the bare zone-center frequency of the E_2(high) phonons. The temperature dependent broadening and shift of the phonon line is described in Eq. (2.1) by the imaginary (Γ) and real part (Δ), respectively, of the complex phonon self-energy: $\Pi(\mathbf{0}j,\omega)=\Delta(\mathbf{0}j,\omega)+i\Gamma(\mathbf{0}j,\omega)$. The linewidth (full width at half maximum) due to the decay of a phonon $(\mathbf{0}j,\omega)$ into a pair of phonons $(\mathbf{q_1}j_1,\omega_1)$ and $(\mathbf{q_2}j_2,\omega_2)$ (three-phonon summation process) is given by[6–9]

$$\begin{aligned}\Gamma(\mathbf{0}j,\omega;T)=&\frac{18\pi}{\hbar^2}\sum_{\mathbf{q},j_1,j_2}|V_3(\mathbf{0}j,\mathbf{q_1}j_1,\mathbf{q_2}j_2)|^2\\&\times[n_{j_1}(\mathbf{q_1};T)+n_{j_2}(\mathbf{q_2};T)+1]\\&\times\delta\{-\omega+\omega_{j1}(\mathbf{q_1})+\omega_{j2}(\mathbf{q_2})\},\end{aligned} \quad (2.2)$$

where $V_3(\mathbf{0}j,\mathbf{q_1}j_1,\mathbf{q_2}j_2)$ are the cubic coefficients in the expansion of the lattice potential in normal coordinates and $n_{j'}(\mathbf{q}';T)=[\exp\{\hbar\tilde{\omega}_{j'}(\mathbf{q}')/k_BT\}-1]^{-1}$ is the phonon occupation number. We assume that the matrix elements are constant within the energy range of interest and do not depend on crystal momentum and branch index. The frequency dependence of the line width is mainly determined by the combined two-phonon density of states $\rho_2(\omega)$, while the temperature dependence of the linewidth is given by the phonon occupation. Furthermore, we assume that the E_2(high) phonon decays into two phonons of the same energy $\omega_{j_1}=\omega_{j_2}=\omega_{E_2}/2$ and branch $j_1=j_2$. Since we study long-wavelength phonons ($\mathbf{q}\approx0$), these two phonons must have opposite wave vectors $\mathbf{q_1}=-\mathbf{q_2}$. With these approximations, Eq. (2.2) can be rewritten as

$$\begin{aligned}\Gamma(\mathbf{0}j,\omega;T)=&\Gamma_{2,3}(\mathbf{0}j,\omega;T)\\=&V^2_{\Gamma_{3;j_2}}[2n_{j_2}(\mathbf{q_{j_2}};T)+1]\rho_2(\omega)\\&+V^2_{\Gamma_{4;j_3}}[3n_{j_3}(\mathbf{q_3};T)+3n^2_{j_3}(\mathbf{q_3};T)+1\rho_3(\omega),\end{aligned} \quad (2.3)$$

where $V_{\Gamma3;j_2}$ denotes the constant matrix element for the three-phonon processes. In the last expression we also include four-phonon summation processes through $V_{\Gamma4;j_3}$, which denotes the corresponding constant matrix element. The conservation of energy and momentum gives for these scattering processes $\omega_{j_3}=\omega_{j_4}=\omega_{j_5}=\omega_{E_2}/3$ and $\mathbf{q_3}+\mathbf{q_4}+\mathbf{q_5}=\mathbf{0}$.

The shift of the phonon frequency due to anharmonic phonon–phonon interactions can be written as[10,11]

$$\begin{aligned}\Delta(\mathbf{0}j,\omega;T)=&\Delta^{(0)}(\mathbf{0}j;T)+\Delta^{(3)}(\mathbf{0}j,\omega;T)\\&+\Delta^{(4)}(\mathbf{0}j,\omega;T)+\ldots.\end{aligned} \quad (2.4)$$

The first term describes the effect of lattice expansion on the phonon frequencies. The following terms quantify the frequency shift due to three- and higher-order phonon scattering processes. These contributions to the frequency shift can, in principle, be determined by perturbation theory or by *ab initio* calculations.[12] However, since $\Delta^{(3)}$ and $\Delta^{(4)}$ correspond to the real part of the phonon self-energy, they can be obtained by a Kramers–Kronig transformation of the imaginary part, which is proportional to $\rho_2(\omega)$ and $\rho_3(\omega)$, respectively. If we assume that the matrix elements are constant, as we have already done above, Eq. (2.4) can be rewritten as

$$\begin{aligned}\Delta(\mathbf{0}j,\omega;T)=&\Delta_{2,3}(\mathbf{0}j,\omega;T)\\=&\Delta^{(0)}(\mathbf{0}j;T)+V^2_{\Delta_{3;j}}[2n_{j'}(\mathbf{q_j}';T)+1]\\&\times\mathrm{KKT}\{\rho_2(\omega)\}+V^2_{\Delta_{4;j}}[3n_{j''}(\mathbf{q}'';T)\\&+3n^2_{j''}(\mathbf{q}'';T)+1]\mathrm{KKT}\{\rho_3(\omega)\},\end{aligned} \quad (2.5)$$

where $V_{\Delta3;j}$ and $V_{\Delta4;j}$ are the constant matrix elements and KKT denotes the Kramers–Kronig transformation.

In contrast to other studies of anharmonic phonon interactions, where phonon–phonon scattering has been the main subject,[8–12] we focus in particular on the first term of Eq. (2.5), which describes the influence of lattice expansion on the phonon frequencies. This effect dominates the temperature shift of the phonon frequencies in bulk GaN as well as in GaN epilayers grown on thermally mismatched substrates. We treat the first term within the Grüneisen approach, e.g., we describe approximately the thermal frequency shift of the phonons in a heteroepitaxially grown layer (where part of the strain is biaxial) only by the change of the lattice volume, but we take into account the actual in- and out-of-plane strain components in the epilayer, $\epsilon_{\mathrm{GaN}\parallel}$ and $\epsilon_{\mathrm{GaN}\perp}$, respectively. (Arguments for this approximation will be given later on in Sec. V C 2). We consider three contributions to the GaN lattice expansion: the relaxation of the GaN layer as well as the intrinsic thermal expansion of GaN and the substrate. According to these parts we distinguish between the growth of the layer at temperature T_g and the sample cooling to the measurement temperature T,

$$\Delta^{(0)}(\mathbf{0}j;T)=\tilde{\Delta}^{(0)}(\mathbf{0}j;T_g)+\tilde{\Delta}^{(0)}(\mathbf{0}j;T_g,T). \quad (2.6)$$

$\tilde{\Delta}^{(0)}(\mathbf{0}j;T_g)$ accounts for GaN growth at T_g on a substrate with a different lattice constant. The lattice mismatch as well as the specific growth modes (e.g., in case of an AlN nucleation layer[4]) may leave a residual strain in the epitaxial layer already at T_g, which results in a shift of the phonon frequency given by

$$\tilde{\Delta}^{(0)}(\mathbf{0}j;T_g)=\omega_{T_g}(\mathbf{0},j)\{\exp[-\gamma_j\epsilon_g]-1\}, \tag{2.7}$$

where γ_j denotes the Grüneisen constant and ϵ_g is the (small) total residual strain in the layer at T_g. We assume that ϵ_g is constant and temperature independent. If the layer is fully relaxed before cooling, $\epsilon_g=0$. In Eq. (2.7), $\omega_{T_g}(\mathbf{0},j)$ describes the phonon frequency shift due to the increase of the lattice volume at T_g caused by the intrinsic thermal expansion of wurtzite GaN and is given by

$$\omega_{T_g}(\mathbf{0},j)=\omega_0(\mathbf{0},j)\exp\left[-\gamma_j\int_0^{T_g}dT'(2\alpha_{\|\mathrm{GaN}}(T')+\alpha_{\perp\mathrm{GaN}}(T'))\right], \tag{2.8}$$

where $\alpha_{\|\mathrm{GaN}}(T)$ and $\alpha_{\perp\mathrm{GaN}}(T)$ are the in-plane and out-of-plane thermal expansion coefficients, respectively.

The second contribution in Eq. (2.6) describes the phonon frequency shift due to the thermal expansion of GaN and the substrate as well as the influence of biaxial strain which arises in the layer during the sample cooling from T_g to T. This contribution can be written in the modified Grüneisen model as

$$\tilde{\Delta}^{(0)}(\mathbf{0}j;T_g,T)=\omega_{T_g}(\mathbf{0},j)\{\exp[-\gamma_j(2\epsilon_{\|\mathrm{GaN}}(T,T_g)+\epsilon_{\perp\mathrm{GaN}}(T,T_g))]-1\}. \tag{2.9}$$

The in-plane strain component ($\epsilon_{\|\mathrm{GaN}}$) is completely determined by the in-plane thermal expansion coefficient of the substrate ($\alpha_{\|\mathrm{substr}}$)

$$\epsilon_{\mathrm{GaN}\|}(T,T_g)=\int_{T_g}^{T}dT'\,\alpha_{\|\mathrm{substr}}(T'). \tag{2.10}$$

The out-of-plane component ($\epsilon_{\perp\mathrm{GaN}}$) is formed by the superposition of the intrinsic thermal contraction of GaN normal to the layer as well as an additional contribution which arises due to the biaxial strain in the heteroepitaxially grown layer and the Poisson effect of the wurtzite GaN lattice ($\epsilon_{\perp}^{(\mathrm{biax})}=\beta\epsilon_{\|}^{(\mathrm{biax})}$, where $\epsilon_{\perp}^{(\mathrm{biax})}$ and $\epsilon_{\|}^{(\mathrm{biax})}$ are the out-off-plane and in-plane biaxial strain components, respectively)

$$\epsilon_{\mathrm{GaN}\perp}(T,T_g)=\int_{T_g}^{T}dT'\,\alpha_{\perp\mathrm{GaN}}(T')+\beta\int_{T_g}^{T}dT'[\alpha_{\|\mathrm{substr}}(T')-\alpha_{\|\mathrm{GaN}}(T')]. \tag{2.11}$$

B. Numerical parameters for the Grüneisen contribution

For the calculation of the temperature shift of the phonon lines, we need the temperature dependencies of the thermal expansion coefficients of wurtzite GaN, 6H–SiC, and Al_2O_3 for $T\to 0$, which are actually unknown. Therefore, we assume that the temperature dependence of these thermal expansion coefficients can be approximately described by the fourth-order polynomial $\alpha=\bar{c}(\Sigma_{i=0}^{4}c_iT^i)$ with $c_0=1.14\times10^{-7}$ K^{-1}, $c_1=6.73\times10^{-8}$ K^{-2}, $c_2=1.27\times10^{-9}$ K^{-3}, $c_3=5.21\times10^{-15}$ K^{-4}, and $c_4=6.77\times10^{-14}$ K^{-5}, if scaled with $\bar{c}$ to the corresponding room temperature values of $\alpha_{\|\mathrm{GaN}}(300\ \mathrm{K})=5.6\times10^{-6}$ K^{-1}, $\alpha_{\perp\mathrm{GaN}}(300\ \mathrm{K})=3.2\times10^{-6}$ K^{-1}, $\alpha_{\|\mathrm{SiC}}(300\ \mathrm{K})=4.2\times10^{-6}$ K^{-1}, and $\alpha_{\|\mathrm{Al_2O_3}}(300\ \mathrm{K})=7.5\times10^{-6}$ K^{-1}.[13] This polynomial approximately describes the thermal expansion of typical III–V and II–IV semiconductors.[14–16] Furthermore, for the Grüneisen constants of GaN, we use $\gamma_{E_2(\mathrm{high})}=1.8$ and $\gamma_{A_1(\mathrm{LO})}=1.2$.[17,18] Finally, we use for the Poisson effect of the GaN lattice $\beta=-2c_{13}/c_{33}=-0.5$,[2,17] where c_{13} and c_{33} are the elastic stiffness constants.

III. SAMPLES AND EXPERIMENTS

Hexagonal GaN layers were grown by plasma-assisted molecular-beam epitaxy (MBE) on (0001) oriented 6H–SiC either directly or on a thin AlN nucleation layer. Furthermore, a thick, high-quality GaN layer was grown by metal-organic vapor-phase epitaxy (MOVPE) on Al_2O_3. Samples grown on the same substrate exhibit a very similar temperature dependence of the frequency shift and half width of the E_2(high)-phonon line. Therefore, in the following we discuss only three characteristic samples. Samples A and B were grown by MBE on SiC and AlN/SiC substrates, respectively, and sample C was grown by MOVPE on sapphire. All layers have wurtzite structure with the *c*-axis normal to the surface. Samples A and C are completely relaxed, whereas sample B is studied in order to explore additional strain of -0.33% in the GaN layer, which is generated by the specific growth mode of GaN on AlN/SiC.[4] In all samples, the free-carrier density is low ($<10^{16}$ cm^{-3}). Therefore, we disregard plasmons and plasmon–phonon coupling.

Polarized Raman spectra were measured in backscattering geometry, allowing for the study of E_2(high) and A_1(LO) vibrations. The experiments were carried out with a *XY*-Dilor triple spectrograph (spectral resolution of about 0.6 cm^{-1}) under optical excitation at 2.41 eV by an Ar^+ laser. The sample temperature was measured by a thermocouple and crosschecked by the temperature dependent frequency of the longitudinal optical phonon line of an undoped Si crystal.[8,9,11] Furthermore, in order to exclude sample heating by laser excitation, the local sample temperature was also checked by measurements of the Stokes to anti-Stokes intensity ratio of the E_2(high) line.

IV. EXPERIMENTAL RESULTS AND DATA TREATMENT

A. Phonon linewidth

Figure 1 shows the temperature dependence of the full width at half maximum [$\Gamma(T)$] of the E_2(high)-phonon line for samples grown on different substrates. At low temperature the linewidth becomes nearly constant. At room and higher temperatures the increase of the linewidth due to sample heating is about the same for all samples. Therefore, we attribute this broadening to the intrinsic three- and four-phonon summation processes in GaN. We take into account only summation processes, since due to the high frequency of optical phonons in GaN only a few phonons are thermally populated and can take part in difference processes at low

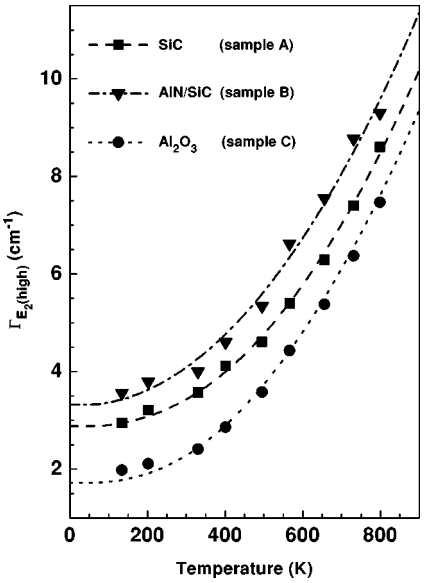

FIG. 1. Measured (points) and fitted (lines) linewidths according to Eqs. (2.3) and (4.1) of the E_2(high)-phonon mode vs temperature for samples A, B, and C. The fit parameters are given in Tables I and II.

temperatures. The measured $\Gamma(T)$ dependencies cannot be well described by Eq. (2.3). However, a good fit is obtained by including additional temperature independent homogeneous (Γ_∞) as well as inhomogeneous contributions (Γ_0) to the linewidth

$$\Gamma^2_{E_2}(T)=\{\Gamma_{2,3}(\mathbf{0}j,\omega;T)+\Gamma_\infty\}^2+\Gamma_0^2. \tag{4.1}$$

From a fit using Eqs. (2.3) and (4.1), we obtain the values for the effective coupling coefficients $V^2_{\Gamma_3;E_2(\mathrm{high})}\rho_2(\omega_{E_2(\mathrm{high})})$ and $V^2_{\Gamma_4;E_2(\mathrm{high})}\rho_3(\omega_{E_2(\mathrm{high})})$ which describe the intrinsic phonon line broadening due to the decay of an E_2(high) phonon into two and three phonons, respectively, as summarized in Table I. The values of Γ_∞ and Γ_0 obtained for samples A, B, and C are listed in Table II. Using these parameters, the calculated linewidths shown in Fig. 1 agree very well with the measured ones. The anharmonicity parameters obtained from the fits of the temperature dependent width of the A_1(LO) phonon line are also shown in Table I. The scattering efficiencies for the other Raman active vibrational modes

TABLE I. Effective coupling parameters (matrix elements times density of states) as well as the bare phonon frequencies (both in cm^{-1}) obtained from the fit of the measured $\Gamma_j(T)$ and $\Delta_j(T)$ dependence of all samples (errors of coupling parameters $\leqslant\pm 20\%$ and of bare phonon frequencies $\leqslant 0.5$ cm^{-1}).

	$j=E_2$(high)	$j=A_1$(LO)
$V^2_{\Gamma_3;j}\rho_2(\omega_j)$	0.42	3.6
$V^2_{\Gamma_4;j}\rho_3(\omega_j)$	0.21	0.2
$V^2_{\Delta_3;j}\rho_2(\omega_j)$	−0.09	−3
$V^2_{\Delta_4;j}\rho_3(\omega_j)$	−0.06	−0.18
$\omega_0\{\mathbf{0},j\}$	569.7	740

TABLE II. Homogeneous and inhomogeneous temperature independent line broadening (Γ_∞ and Γ_0 in cm^{-1}) as well as total unrelaxed strain at T_g (ϵ_g in %) for sample A (grown on SiC), B (AlN/SiC), and C (Al_2O_3) (errors $\leqslant\pm 20\%$).

Sample	A	B	C
Γ_∞	0.6	1.6	0
Γ_0	2.6	2.5	1.6
ϵ_g	0	−0.33	0

are too low or these Raman lines are superimposed by strong lines from the substrate which prevents a precise determination of their anharmonic parameters.

B. Phonon frequency shift

Figure 2 shows the temperature dependence of the frequency shift $[\Delta(T)]$ of the E_2(high) phonons for samples A, B, and C. For $T\rightarrow 0$ the phonon frequency becomes nearly constant. At room and higher temperatures the frequency shifts for samples A (SiC substrate) and B (AlN/SiC) are nearly the same, but the absolute value for sample B is about 3.5 cm^{-1} larger (than that of sample A). The $\Delta(T)$ dependence for sample C (Al_2O_3) is different from that of samples A and B. From a second-order polynomial fit to these experimental data we obtain the frequencies of the E_2(high) phonons in the GaN layers grown on SiC and Al_2O_3 substrates at low, room, and at the growth temperature as listed in Table III. This fit shows that the difference between the E_2(high)-phonon frequencies of layers grown on Al_2O_3 and on SiC is 3.1 cm^{-1} at room temperature and reduces to 1.3 cm^{-1} at the growth temperature T_g. This small frequency difference at $T_g\approx 1000$ K (Fig. 2) indicates that samples A and C are almost relaxed at T_g. Therefore, we neglect this small residual strain, i.e., we disregard Eq. (2.7) for samples A and C and fit Eq. (2.5) by using Eq. (2.6) and Eqs. (2.8)–(2.11) and the thermal expansion coefficients given

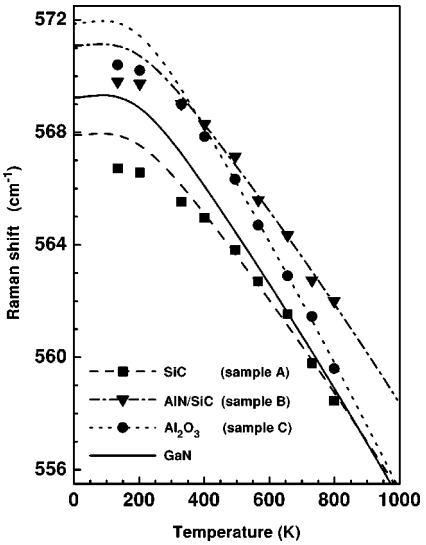

FIG. 2. Measured Raman shift of the E_2(high) phonons for samples A, B, and C. The lines show the fitted phonon frequencies for bulk GaN and for the GaN layers on the different substrates.

TABLE III. Frequencies of E_2(high) phonons (in cm^{-1}) in GaN layers grown on different substrates at low, room, and at the layer growth temperature obtained from a fit of the measured $\Delta(T)$ dependence using a second order polynomial. The frequencies of bulk GaN derived from our model are also listed (frequency error $\leqslant \pm 0.5$ cm^{-1}, temperature error $\leqslant \pm 10$ K). GaN layers in Refs. 21 and 22 were grown by MBE on α-Al_2O_3 substrates with 200–400 and 50–70 μm, respectively, thick GaN buffer layers grown by hydride–vapor-phase epitaxy. Due to the thick GaN buffer layers, these samples can be assigned to be in between layers grown on Al_2O_3 substrate and bulk GaN.

	GaN grown on			Bulk
T(K)	SiC	AlN/SiC	Al_2O_3	GaN
6	566.6	570.1	571.2[a,b]	569.6[a,c]
300	566.0[d]	569.0[e]	569.1[f,g]	567.9[g,h]
990	552.5	556.9	553.8	555.3

[a]569 cm^{-1}, Ref. 22.
[b]569.2 cm^{-1}, Ref. 26 ($Ga^{14}N$).
[c]Calculated values: 565 cm^{-1}, Ref. 22; 579 cm^{-1}, Refs. 23,26; 558 cm^{-1}, Ref. 28; 560 cm^{-1}, Ref. 29.
[d]564,7 cm^{-1}, Ref. 2; 565.5–568 cm^{-1}, Ref. 3; 564.9 cm^{-1}, Ref. 4.
[e]568.9 cm^{-1}, Ref. 4.
[f]570.7 cm^{-1}, Ref. 2; 570.5–572 cm^{-1}, Ref. 3; 569 cm^{-1}, Ref. 27.
[g]569 cm^{-1}, Ref. 21; 567.6 cm^{-1}, Ref. 22.
[h]5662 cm^{-1}, Ref. 2; 568 cm^{-1}, Ref. 17.

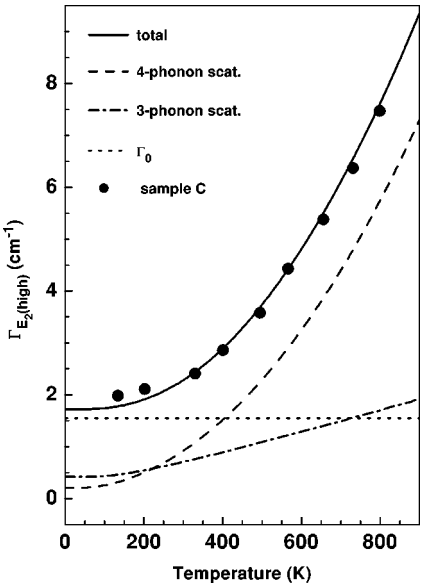

FIG. 3. Effect of three- and four-phonon summation processes as well as inhomogeneous broadening and total linewidth of the E_2(high)-phonon mode in GaN grown on Al_2O_3 (sample C) calculated by Eqs. (2.3) and (4.1). Solid squares show the experimental results.

in Sec. II B to the measured $\omega_{E_2(T)}$ data. From this procedure, we obtain the $V^2_{\Delta_3;E_2(\mathrm{high})}\rho_2(\omega_{E_2(\mathrm{high})})$ and $V^2_{\Delta_4;E_2(\mathrm{high})}\rho_3(\omega_{E_2(\mathrm{high})})$ values as well as the bare phonon frequency. These data are given in Table I, and the fitted curves are shown in Fig. 2. For layer B (GaN on AlN/SiC), Fig. 2 shows a nearly constant frequency offset of about 3.3 cm^{-1} with respect to the layer A (bare SiC substrate), which gives according to Eq. (2.7) a residual strain at T_g as listed in Table II. The anharmonicity parameters of the A_1(LO)-vibrational mode are also listed in Table I.

V. DISCUSSION

A. Three- and four-phonon summation processes

For $T \to 0$ phonons are thermally unoccupied. The linewidth becomes temperature independent and its value is given by the zero-point lattice vibrations (apart from temperature independent contributions, Sec. V A). The *intrinsic* E_2(high)-phonon–phonon scattering in GaN is most clearly observable at room and higher temperatures in the same increase of the linewidth with sample heating independently of the substrate (Fig. 1). In particular the intrinsic anharmonicity [Eq. (2.3)] can be well studied in the $\Gamma(T)$ dependence of sample C, since it exhibits the smallest $\Gamma_0^2+\Gamma_\infty^2$ value of our layers studied (Table II). Figure 3 shows the different contributions to the linewidth for this sample calculated using the parameters of Tables I and II. It can be clearly seen that three-phonon summation processes contribute only weakly to the temperature broadening of the E_2(high)-phonon line. This behavior is already expected from the obtained small value of $V^2_{\Gamma_3;E_2(\mathrm{high})}\rho_2(\omega_{E_2(\mathrm{high})})$ in Table I, which is about one order smaller than those of other typical semiconductors.[8,9,11] In contrast, the value of $V^2_{\Gamma_4;E_2(\mathrm{high})}\rho_3(\omega_{E_2(\mathrm{high})})$ for four-phonon scattering processes is similar to that of other semiconductors.

From a Taylor expansion of Eq. (4.1) using Eq. (2.3) and the fit parameters of Tables I and II, we obtain a general expression for the E_2(high)-phonon linewidth of GaN:

$$\Gamma^2_{E_2(\mathrm{high})} \approx \Gamma_0^2 + (\Gamma_\infty + 0.63\,\mathrm{cm}^{-1} + 5.84\times 10^{-4}\,\mathrm{cm}^{-1}\,\mathrm{K}^{-1}T + 1.01\times 10^{-5}\,\mathrm{cm}^{-1}\,\mathrm{K}^{-2}T^2)^2. \quad (5.1)$$

The resulting *intrinsic* width of the E_2(high)-Raman line at low and room temperature is 0.63 and 1.7 cm^{-1}, respectively. These values are comparable with those of the longitudinal optical zone-center phonons in InP (Ref. 19) and Ge.[20] In order to explain this small linewidth (or the small amount of three-phonon scattering processes), we have reproduced in Fig. 4(a) the phonon dispersion calculated by Siegle *et al.*[21] using a modified valence-force model. From this dispersion, which agrees well with that of other calculations,[22–25] we estimate the two-phonon density of states by interpolating between the different branches of the high-symmetric directions in the Brillouin zone and taking into account the degeneracy of the vibrational modes. The approximated two-phonon density of states for summation processes is shown in Fig. 4(b). Around the E_2(high)-phonon energy, the two-phonon density is small, since these phonons can decay only into two phonons at the K point in the Brillouin zone (with $\omega=\omega_{E_2(\mathrm{high})}/2$ as assumed in Sec. II A). Therefore, the E_2(high) phonons in GaN have a relatively long lifetime and a small linewidth. Assuming constant matrix elements, we conclude from the $\rho_2(\omega)$ data in Fig. 4(b), that the linewidth of the higher-frequency A_1(LO)- and E_1(LO)-phonon modes should be about four times larger than that of the E_2(high)-vibrational mode. This prediction has been confirmed by our experimental results. The anharmonicity parameter for three-phonon scattering

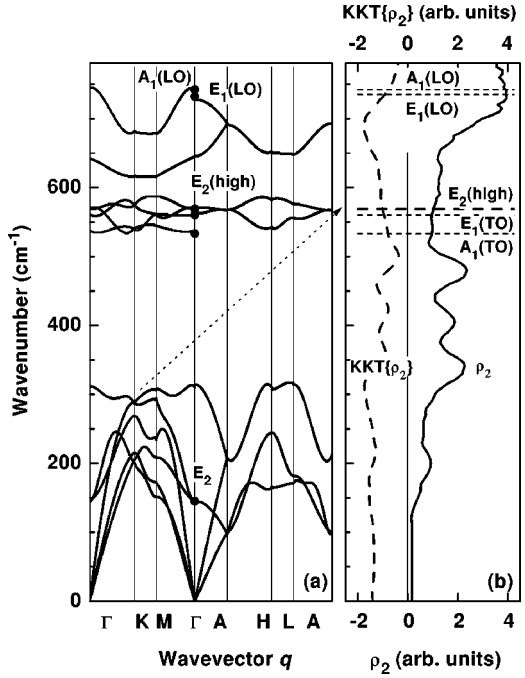

FIG. 4. (a) Phonon dispersion of hexagonal GaN by Siegle *et al.* (Ref. 21) and (b) calculated density of states for two-phonon summation processes [$\rho_2(\omega)$, solid line] as well as its Kramers–Kronig transformed [KKT $\{\rho_2(\omega)\}$, dashed line].

$[V^2_{\Gamma_3;A_1(\mathrm{LO})}\rho_2(\omega_{A_1(\mathrm{LO})})]$ is actually much larger than that for the E_2(high)-phonon decay as shown in Table I. The corresponding value for four-phonon summation processes is of the same order as that for the E_2(high)-phonon decay.

For a discussion of the frequency shift, Fig. 4(b) also shows the Kramers–Kronig transformed of the density of states for two-phonon summation processes [cf. Eq. (2.5)]. Due to the small amount of three-phonon scattering processes we expect that the decay into two phonons influences the temperature shift of the E_2(high) phonons only weakly. Figure 5 confirms that this contribution to the temperature shift of the phonon frequency is actually small. From the

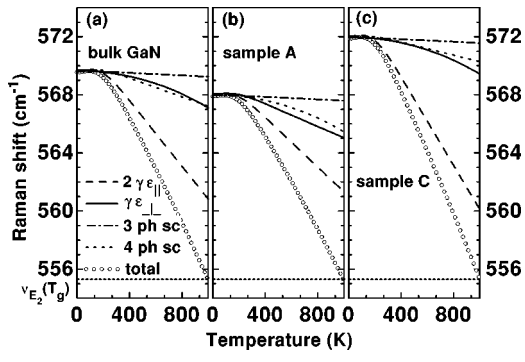

FIG. 5. Contributions to the temperature shift of the E_2(high)-phonon mode of: (a) bulk GaN, (b) GaN grown on SiC (sample A), and (c) GaN grown on Al_2O_3 substrate (sample C). The phonon frequency at T_g [Eq. (2.8)] is denoted by a horizontal thin short-dashed line. The influence of the total in-plane strain [Eqs. (2.9) and (2.10)] is shown by dashed lines and that of the out-of-plane strain [Eq. (2.9) and (2.11)] by solid lines. Three- and four-phonon summation processes are denoted by dashed-dotted and dotted, respectively, lines. The total linewidth is given by circles.

KKT$\{\rho_2(\omega)\}$ curve in Fig. 4(b) we would expect that the effect of three-phonon processes on the temperature shift of the A_1(LO) phonons should be comparable to that of the E_2(high) phonons. However, Table I reveals that the value of $V^2_{\Gamma_4;A_1(\mathrm{LO})}\rho_3(\omega_{A_1(\mathrm{LO})})$ is much larger. This discrepancy may be due to an incorrect value of the Grüneisen constant of the A_1(LO)-vibrational mode or a frequency dependence of the matrix elements, which we neglected in our model.

B. Temperature independent line broadening contributions

In our model the temperature independent contributions to the linewidth are characterized in Eq. (4.1) by $\Gamma^2_\infty+\Gamma^2_0$. GaN layers contain numerous defects, which cause a partial relaxation of the crystal momentum conservation for phonon–phonon scattering processes. As a consequence, the increasing rate of higher-order phonon scattering and the loss of coherence lead to a temperature-independent, but homogeneous line broadening characterized by Γ_∞. Table II shows that the value of Γ_∞ vanishes for the 3.5 μm thick layer C. This indicates the relatively small average density of lattice defects present in thick, high-quality GaN layers grown by MOVPE on sapphire. However, for the GaN layers grown on SiC, we obtain $\Gamma_\infty>0$, which reflects the higher average defect density in the 1 μm thick layers.

Heteroepitaxially grown GaN layers are subject to strain. Due to the lattice mismatch and depending on the nucleation mechanism, inhomogeneously distributed strain fields are formed at the layer/substrate interface. Due to dislocations, voids, a.s.o. these randomly distributed strain fields decrease about inversely proportional with the distance from the layer/substrate interface. Therefore, for heteroepitaxially grown GaN layers, with increasing layer thickness, the part of the layer which is inhomogeneously strained decreases with respect to the homogeneously strained contribution and, therefore, the phonon linewidth decreases.[1] In our model, this inhomogeneous line broadening is characterized by Γ_0. Whereas the GaN layer in sample C (Al_2O_3 substrate) is 3.5 μm thick, the layers in samples A and B (SiC and AlN/SiC substrates, respectively) are about 1 μm thick, which explains the comparatively large Γ_0 values for samples A and B (Table II). The Γ_0 values for samples A and B are almost the same, which reflects the comparable inhomogeneous strain at the layer/substrate and layer/AlN/substrate interfaces of samples A and B, respectively. An additional homogenous strain, e.g., due to the AlN nucleation layer, does not influence Γ_0.

It is worth mentioning that for thin GaN layers with large inhomogeneous strain and a high defect density, the values of Γ_0 and Γ_∞ of Table II increase by as much as 1 cm^{-1}. Summarizing, the lattice mismatch between GaN and the substrate and certain growth modes cause defects in the epilayers, which reduce the phonon lifetime of all vibrational modes. $\Gamma^2_\infty+\Gamma^2_0$ is a measure for the crystalline quality of the epilayers, which can be accurately measured only at low temperature, where the line broadening due to the temperature dependent phonon–phonon scattering disappears.

C. Grüneisen effect

1. Intrinsic thermal lattice expansion of GaN

In the following, we will show that the temperature dependence of the phonon frequency (Fig. 2) is governed mainly by the lattice expansion. Therefore, we consider at first the *intrinsic* Grüneisen effect for bulk or homoepitaxial grown GaN, which we obtain from Eqs. (2.10) and (2.11) if α_{substr} is replaced by α_{GaN}. Figure 5(a) shows the calculated Grüneisen contribution for GaN by using the thermal expansion parameters given in Sec. II B and the fit parameters contained in Table I. The phonon frequencies become constant at low temperature, since $\alpha_{\mathrm{GaN}}(T\rightarrow 0)\rightarrow 0$. At room and higher temperatures the shift of the E_2(high)-phonon frequency in GaN is dominated by the Grüneisen contribution, which is about three times larger than that of phonon scattering (see Sec. IV A). The Grüneisen effect is determined mainly by the in-plane thermal lattice expansion [Eq. (2.10); dashed line in Fig. 5(a)] which is about three times larger than the out-of-plane part [Eq. (2.11); Fig. 5(a) solid line]. This phenomenon results, first, from the relation that $\alpha_{\parallel} > \alpha_{\perp}$ and, second, from the fact that two in-plane but only one out-of-plane component contribute to the volume change.

Table III contains the frequencies of the E_2(high) phonons derived from our model for bulk GaN at low, room, and at the growth temperature (by taking into account the thermal lattice expansion as well as phonon–phonon scattering). Davidov *et al.*[22] measured the Raman scattering of GaN layers, which were grown by MBE not directly on sapphire but on a 50–70 μm thick GaN buffer layer. This buffer layer was grown by hydride–vapor-phase epitaxy on Al_2O_3. Therefore, these samples can be assigned to be in between heteroepitaxy and homoepitaxy. The E_2(high)-phonon frequency of these layers at low temperature is, indeed, in between our values for GaN layers grown on sapphire and bulk samples (Table III). Furthermore, our value of the E_2(high)-phonon frequency in bulk GaN at low temperature agrees well with the average value of the frequencies calculated by Karch *et al.*,[23] Zhang *et al.*,[26] Gorczyca *et al.*,[28] and Miwa and Fukumoto,[29] where the scattering of the theoretical data is large due to the different *ab initio* approaches. More reliable frequency data are published for the E_2(high) phonons in bulk GaN at room temperature. Our value (Table III) agrees well with measurements of Kisielowski *et al.*[2] and Perlin *et al.*[17] The frequencies obtained by Siegle *et al.*[21] and Davidov *et al.*[22] for GaN layers grown on thick GaN buffer layers on sapphire substrates are in between our obtained values for layers on Al_2O_3 and bulk GaN.

Our measured temperature shift of the E_2(high) phonons in bulk GaN can be described approximately by the polynomial $\Delta_{E_2(\mathrm{high})}=a_0+a_1(T-T_0)+a_2(T-T_0)^2$, where the coefficients a_0–a_2 for room ($T_0=300$ K) and higher temperatures are given in Table IV. The linear term is predominantly governed by the Grüneisen effect, whereas the quadratic term is determined essentially by the intrinsic phonon–phonon scattering.

TABLE IV. Coefficients of the second-order polynomial $\Delta_{E_2(\mathrm{high})}=a_0+a_1(T-T_0)+a_2(T-T_0)^2$, ($T_0=300$ K) which describes the $\Delta_{E_2(\mathrm{high})}(T)$ dependence for $T>300$ K for bulk GaN and for samples A (GaN grown on SiC) and C (Al_2O_3). The coefficient a_0 is given in cm^{-1}, a_1 in $\mathrm{cm}^{-1}\,\mathrm{K}^{-1}$, and a_2 in $\mathrm{cm}^{-1}\,\mathrm{K}^{-2}$. ($a_0$ error$\leqslant\pm 0.5$ cm^{-1}, a_1 and a_2 errors $\leqslant\pm 10\%$).

	Bulk GaN	GaN grown on	
		SiC	Al_2O_3
a_0	567.5	565.6	568.7
a_1	-0.0164	-0.0129	-0.0214
a_2	-2.84×10^{-6}	-2.84×10^{-6}	-2.84×10^{-6}

2. Substrate induced strain

Figure 2 shows that the *external* influence of different substrates results in different redshifts of the E_2(high) phonons with sample heating (for $T\geqslant 300$ K). Table III shows the frequencies obtained from a model-independent second-order fit of the measured $\omega_{E_2(\mathrm{high})}(T)$ dependencies for layers grown on SiC, AlN, and Al_2O_3 substrates at low, room, and at the growth temperature. These values agree well with published data.[2–4,21–23,26–29]

In the following, we analyze the influence of biaxial strain on the E_2(high)-phonon frequency (Sec. II A). The values of the thermal expansion coefficients of SiC and Al_2O_3 are about $\mp 30\%$, respectively, different from that of bulk GaN. Therefore, about 70% of the thermal expansion of the heteroepitaxially grown GaN layers agree with that of bulk GaN (Sec. V C 1). The residual part of 30% causes biaxial strain in the epilayers. Usually, the influence of biaxial strain on the phonon frequency is described by a superposition of hydrostatic and uniaxial strain.[4] However, this treatment requires the value of the optical deformation potential constant for uniaxial strain, which is actually unknown in the case of GaN. For hexagonal lattices, (biaxial or) uniaxial strain along the *c* axis does not change the lattice symmetry. The twofold degeneracy of the E_2(high)-lattice mode is not lifted and no line splitting occurs. Therefore, in our approximation (Sec. II A), we describe the shift of the phonon frequency due to biaxial strain by a slightly modified Grüneisen approach, where instead of the hydrostatic strain, the actual change of the lattice volume is taken into account [cf. Eqs. (2.9)–(2.11)]. We obtain within a linear approximation for the case of pure biaxial strain due to the Poisson effect of the lattice $\Delta^{(\mathrm{biax})}_{E_2(\mathrm{high})}\approx\gamma_{E_2}\omega_{0,E_2}(2\epsilon_{\parallel}+\epsilon_{\perp})=\gamma_{E_2}\omega_{0,E_2}\epsilon_{\perp}(2/\beta+1)=3024\ \mathrm{cm}^{-1}\epsilon_{\perp}$, where β was given in Sec. II B. This frequency shift due to biaxial strain is only slightly larger than that measured by Kisielowski *et al.* ($\Delta^{(\mathrm{biax})}_{E_2(\mathrm{high})}=2630\ \mathrm{cm}^{-1}\epsilon_{\perp}$) and Klose *et al.* ($\Delta^{(\mathrm{biax})}_{E_2(\mathrm{high})}=2537\ \mathrm{cm}^{-1}\epsilon_{\perp}$). Therefore, in the case of the E_2(high) mode the influence of a uniaxial deformation potential is sufficiently well taken into account in our approximation. The advantage of the modified Grüneisen model is that Eqs. (2.10) and (2.11) explicitly the unknown uniaxial deformation potential constant do not contain.

Figure 2 shows that temperature shifts of the E_2(high)-phonon frequency for layers grown on SiC, AlN/SiC, and Al_2O_3 substrates calculated by taking into account thermal lattice expansions and biaxial strain as discussed

above. The obtained values agree well with the measured ones. The deviations at low temperatures, where the anharmonicity disappears, may be caused by the approximations used in the temperature dependence of the thermal expansion coefficients (cf. Sec. II B).

Figures 5(b) and 5(c) show the different contributions to the phonon frequency shift for the layers grown on SiC and Al_2O_3 substrates, respectively. The temperature dependent change of the GaN lattice, and therefore the phonon shift, is determined mainly by the in-plane thermal expansion coefficient of the corresponding substrate [see, Eqs. (2.9) and (2.10)]. For SiC, the in-plane thermal contraction [Fig. 5(b), dashed line] is smaller than for Al_2O_3 substrates [Fig. 5(c), dashed line]. The in-plane contraction for bulk GaN lies between both heteroepitaxial cases [Fig. 5(a), dashed line], which reflects the well-known compressive or tensile strain in the case of SiC or Al_2O_3 substrates, respectively (at $T < T_g$).

3. Relaxation state at growth temperature

Finally, we consider the relaxation state of heteroepitaxial GaN layers at growth temperature T_g. A measure for the lack of relaxation at T_g is ϵ_g in Eq. (2.6). A noncomplete relaxation results in a phonon frequency, which is different from that of bulk GaN at $T_g \approx 1000$ K. Figure 2 reveals for GaN films grown on a thin pseudomorphic AlN nucleation layer on SiC a nearly constant frequency offset of about 3.3 cm^{-1} with respect to the layer on the bare SiC substrate. This frequency shift can be explained by an additional strain of $\epsilon_g = -0.33\%$ due to the specific growth mode of GaN on AlN/SiC substrates.[4]

VI. CONCLUSIONS

The temperature dependent broadening of the E_2(high)-phonon Raman line from GaN layers is essentially governed by intrinsic properties, namely phonon–phonon scattering. The intrinsic linewidth of the E_2(high) phonons at low and room temperatures is determined to be 0.63 and 1.7 cm^{-1}. This small linewidth is caused by the rather small value of the two-phonon density of states, whereas the stronger decay of A_1(LO) phonons by three-phonon processes leads to a four times larger linewidth. Substrate-induced inhomogeneous strain and lattice defects in the GaN layers lead to the temperature-independent phonon line broadening $\Gamma_0^2 + \Gamma_\infty^2$. This contribution to the linewidth serves as a measure for the layer quality. Frequently, its value is comparable with the intrinsic E_2(high)-phonon linewidth at room temperature. Therefore, $\Gamma_0^2 + \Gamma_\infty^2$ can be determined accurately only at low temperatures.

The frequency of the bare E_2(high) phonons in (bulk) GaN is determined to be 569.7 cm^{-1}. The redshift of the phonon lines with sample heating is essentially caused by the thermal expansion of the hexagonal GaN lattice and only weakly influenced by phonon scattering. For heteroepitaxially grown GaN layers the temperature dependent phonon shift is strongly influenced by the in-plane thermal expansion of the substrate. This effect on the E_2(high) phonons can be approximated by a modified Grüneisen model which takes into account the thermal in-plane strain in the layer due to the substrate and the out-of-plane strain due to the thermal expansion of GaN itself, as well as the tetragonal distortion of the GaN lattice due to the biaxial strain. The difference between the E_2(high)-phonon frequencies of heteroepitaxially grown layers and bulk GaN at the growth temperature is a measure of the degree of relaxation of the layer.

ACKNOWLEDGMENTS

The authors would like to thank P. Santos and H. T. Grahn for helpful discussion and a critical reading of the manuscript.

[1] T. Kozawa, T. Kachi, H. Kano, H. Nagase, N. Koide, and K. Manabe, J. Appl. Phys. **77**, 4389 (1995).
[2] C. Kisielowski *et al.*, Phys. Rev. B **54**, 17745 (1996).
[3] M. Klose, N. Wieser, G. C. Rohr, R. Dassow, F. Scholz, and J. Off, J. Cryst. Growth **189/190**, 634 (1998).
[4] P. Waltereit, O. Brandt, A. Trampert, M. Ramsteiner, M. Reiche, M. Qi, and K. H. Ploog, Appl. Phys. Lett. **74**, 3660 (1999).
[5] M. Giehler, M. Ramsteiner, O. Brandt, H. Yang, and K. H. Ploog, Appl. Phys. Lett. **67**, 733 (1995).
[6] A. A. Maradudin and A. E. Fein, Phys. Rev. **128**, 2589 (1962).
[7] R. A. Cowley, J. Phys. (Paris) **26**, 659 (1965).
[8] M. Balkanski, R. F. Wallis, and E. Haro, Phys. Rev. B **28**, 1928 (1983); **29**, 2051 (1984).
[9] J. Menendéz and M. Cardona, Phys. Rev. B **29**, 2051 (1984).
[10] P. G. Klemens, Phys. Rev. **148**, 845 (1966).
[11] T. R. Hart, R. L. Aggrawal, and B. Lax, Phys. Rev. B **1**, 638 (1970).
[12] A. Debernardi, Phys. Rev. B **57**, 12847 (1998).
[13] H. Morkoç, S. Strite, G. B. Gao, M. E. Lin, B. Sverdlov, and M. Burns, J. Appl. Phys. **76**, 1363 (1994).
[14] T. Soma, Y. Saitoh, and H. Matsuo, Solid State Commun. **42**, 889 (1982).
[15] T. Soma, Solid State Commun. **34**, 927 (1980).
[16] J. Xie, S. P. Chen, J. S. Tse, S. Gironoli, and S. Baroni, Phys. Rev. B **60**, 9444 (1999).
[17] P. Perlin, C. Jaubertie-Carillon, J. P. Itie, A. S. Miguel, I. Grzegory, and A. Polian, Phys. Rev. B **45**, 83 (1992).
[18] K. Kim, W. R. L. Lambrecht, and B. Segall, Phys. Rev. B **53**, 16310 (1996).
[19] G. Irmer, M. Wenzel, and J. Monecke, Phys. Status Solidi B **195**, 85 (1996).
[20] J. M. Zhang, M. Giehler, A. Göbel, T. Ruf, M. Cardona, E. E. Haller, and K. Itoh, Phys. Rev. B **57**, 1348 (1998).
[21] H. Siegle, G. Kaczmarczyk, L. Filippidis, A. P. Litvinchuk, A. Hoffmann, and C. Thomsen, Phys. Rev. B **55**, 7000 (1997).
[22] V. Yu. Davidov, Yu. E. Kitaev, I. N. Goncharik, and A. N. Smirnov, Phys. Rev. B **58**, 12899 (1998).
[23] K. Karch, J. M. Wagner, and F. Bechstedt, Phys. Rev. B **57**, 7043 (1998).
[24] J. C. Nipko, C.-K. Loong, C. M. Balkas, and R. F. Davis, Appl. Phys. Lett. **73**, 34 (1998).
[25] K. Parlinski and Y. Kawazoe, Phys. Rev. B **60**, 15511 (1999).
[26] J. M. Zhang, T. Ruf, M. Cardona, O. Ambacher, M. Stutzmann, J.-M. Wagner, and F. Bechstedt, Phys. Rev. B **56**, 14399 (1997).
[27] T. Azuhata, T. Sota, K. Suzuki, and S. Nakamura, J. Phys. C **7**, L129 (1995).
[28] I. Gorczyca, N. E. Cristensen, E. L. Peltzer y Blancá, and C. O. Rodriguez, Phys. Rev. B **51**, 11936 (1995).
[29] K. Miwa and A. Fukumoto, Phys. Rev. B **48**, 7897 (1993).